

Rotation to Sparse Loadings using L^p Losses and Related Inference Problems

Xinyi Liu, Gabriel Wallin, Yunxiao Chen, and Irini Moustaki

London School of Economics and Political Science

Abstract

Exploratory factor analysis (EFA) has been widely used to learn the latent structure underlying multivariate data. Rotation and regularised estimation are two classes of methods in EFA that are widely used to find interpretable loading matrices. This paper proposes a new family of oblique rotations based on component-wise L^p loss functions ($0 < p \leq 1$) that is closely related to an L^p regularised estimator. Model selection and post-selection inference procedures are developed based on the proposed rotation. When the true loading matrix is sparse, the proposed method tends to outperform traditional rotation and regularised estimation methods, in terms of statistical accuracy and computational cost. Since the proposed loss functions are non-smooth, an iteratively reweighted gradient projection algorithm is developed for solving the optimisation problem. Theoretical results are developed that establish the statistical consistency of the estimation, model selection, and post-selection inference. The proposed method is evaluated and compared with regularised estimation and traditional rotation methods via simulation studies. It is further illustrated by an application to big-five personality assessment.

Keywords: Component loss function, analytic rotation, regularised estimation, model selection, post-selection inference

1 Introduction

Exploratory Factor Analysis (EFA) has been widely used to learn the latent structure underlying multivariate data. A major problem in EFA is to identify an interpretable factor structure among infinitely many equivalent solutions that give the same data distribution, where two equivalent solutions differ by a rotation transformation (see chapters 10-12, Mulaik, 2009). Mathematically, one aims to find a sparse solution for which many entries of the loading matrix are exactly or approximately zero, so that each factor can be interpreted based on a small number of manifest variables whose loadings on the factor are not close to zero. This idea dates back to the seminal discussion on simple factor structure in Thurstone (1947).

Methods for obtaining sparse loading structures can be classified into two categories – rotation and regularised estimation methods. A rotation method involves two steps. In the first step, an estimate of the loading matrix is obtained. Typically, but not necessarily, a maximum likelihood estimator is used in this step (Bartholomew et al., 2011), under some arbitrary but mathematically convenient constraints that avoid the rotational indeterminacy. In the second step, one rotates the estimated loading matrix to minimise a certain loss function that measures the sparsity level of the rotated solution¹, where a smaller loss function

¹Rotation methods that solve maximisation problems can always be reformulated to solve minimisation problems.

value indicates a more sparse solution. Different rotation methods have been proposed that differ by first, whether the factors are allowed to be correlated and second the loss function for measuring sparsity. A rotation method is called an orthogonal rotation when the factors are constrained to be uncorrelated, and an oblique rotation, otherwise. Different loss functions have been proposed for orthogonal and oblique rotations, including varimax (Kaiser, 1958), oblimin (Jennrich & Sampson, 1966), geomin (Yates, 1987), simplimax (Kiers, 1994), componentwise loss (Jennrich, 2004, 2006), among many others. Among the existing rotation methods, we draw attention to the monotone concave Component Loss Functions (CLFs; Jennrich, 2004, 2006) due to their desired theoretical properties and superior performance in recovering sparse loading matrices. Specifically, (Jennrich, 2004, 2006) provided some theoretical guarantees to the CLFs when the true loading matrix has a perfect simple structure and further found that the CLFs are often more accurate in recovering sparse loading matrices than other rotation methods, under both orthogonal and oblique settings.

In recent years, several regularised estimation methods have been proposed for EFA (e.g., Geminiani et al., 2021; Jin et al., 2018; Trendafilov, 2014; Yamamoto et al., 2017). Slightly different from rotation methods, a regularised estimation method simultaneously performs parameter estimation and model selection. It introduces a LASSO-type sparse-inducing regularisation term into the loss function for parameter estimation, where the regularisation term imposes sparsity on the estimated loading. It typically obtains a sequence of candidate models by varying the weight of the regularisation term in the loss function. The final model is chosen from the candidate models, often using an information criterion.

This paper proposes a new family of oblique rotations based on component-wise L^p loss functions, for $0 < p \leq 1$. The proposed loss functions are shown to be special cases of monotone concave CLFs and thus share the same theoretical properties. We note that Jennrich (2004, 2006) considered the L^1 loss function but not the L^p loss functions with $p < 1$. With the proposed rotations, we answer several previously unaddressed questions regarding rotation and regularised estimation methods. First, we establish the statistical consistency of the rotated solution. More specifically, we provide conditions under which the rotated solution converges to the true sparse loading matrix as the sample size goes to infinity. These conditions also provide insights into the choice of p . Seemingly straightforward, this consistency result requires some refined analysis and, to our best knowledge, such results have not been established for other rotation methods. In particular, the theoretical results for the CLFs in Jennrich (2004, 2006) were established with respect to the population loading matrix rather than its estimate. Second, do regularised estimation methods outperform rotation methods, or vice versa? To obtain some insights into this question, we show that the proposed rotation method can be viewed as the limiting case of a regularised estimator when the weight of the regularisation term converges to zero. In addition, to compare the two methods in terms of their performance in model selection, we develop a hard-thresholding procedure that conducts model selection based on a rotated solution. Through computational complexity analysis and simulation studies, it is found that rotation achieves similar statistical accuracy as regularised estimation, but with a lower computational cost. Third, monotone concave CLFs, including the proposed L^p loss functions, are not smooth everywhere. Consequently, the traditional gradient projection algorithms are no longer applicable. Jennrich (2004, 2006) bypassed the computational issue by replacing a CLF with a smooth approximation, but also pointed out potential issues with this treatment. We propose an Iteratively Reweighted Gradient Projection (IRGP) algorithm that may better solve this nonsmooth optimisation problem. Finally, uncertainty quantification for the rotated solution affects the interpretation of the factors and, thus, is vital in EFA. However, the delta method, which is used to obtain confidence intervals for rotation methods with a smooth objective function (Jennrich, 1973), is not applicable due to the non-smoothness of the current loss functions. That is, the delta method requires

the loss function to be smooth at the true loading matrix, which is not satisfied for monotone concave CLFs. We tackle this problem by developing a post-selection inference procedure that gives asymptotically valid confidence intervals for loadings in a rotated solution. The proposed method is evaluated and compared with regularised estimation and traditional rotation methods via simulation studies. The proposed method is further illustrated by an application to big-five personality assessment.

The rest of the paper is structured as follows. Section 2 proposes L^p criteria for oblique rotation, and draws a connection with regularised estimation. Section 3 discusses statistical inferences based on the proposed rotation method and establishes their asymptotic properties, and Section 4 develops an iteratively reweighted gradient projection algorithm for solving the optimisation problem associated with the proposed rotation criteria. The proposed method is evaluated via simulation studies in Section 5 and an application to big-five personality assessment in Section 6. We conclude this paper with discussions on the limitations of the proposed method and future directions in Section 7. Proof of the theoretical results and additional details about the simulation and real application are given in the supplementary material.

2 L^p Rotation Criteria

2.1 Problem Setup

We consider an exploratory linear factor model with J indicators and K factors given by

$$\mathbf{X}|\boldsymbol{\xi} \sim \mathcal{N}(\boldsymbol{\Lambda}\boldsymbol{\xi}, \boldsymbol{\Omega}), \quad (1)$$

where \mathbf{X} is a J -dimensional vector of manifest variables, $\boldsymbol{\Lambda} = (\lambda_{jk})_{J \times K}$ is the loading matrix, $\boldsymbol{\xi}$ is a K -dimensional vector of common factors, and $\boldsymbol{\Omega} = (\omega_{ij})_{J \times J}$ denotes the residual covariance matrix. It is assumed that the common factors are normally distributed with variances fixed to 1, i.e., $\boldsymbol{\xi} \sim \mathcal{N}(\mathbf{0}, \boldsymbol{\Phi})$, where $\boldsymbol{\Phi} \in \mathbb{R}^{K \times K}$ has diagonal entries ϕ_{kk} , $k = 1, \dots, K$, equal to 1 and is symmetric positive definite, denoted by $\boldsymbol{\Phi} \succ 0$. The manifest variables are assumed to be conditionally independent given $\boldsymbol{\xi}$, i.e., the off-diagonal entries of $\boldsymbol{\Omega}$ are set to 0. To simplify the notation, we use $\boldsymbol{\theta} = (\boldsymbol{\Lambda}, \boldsymbol{\Phi}, \boldsymbol{\Omega})$ to denote all of the unknown parameters. The model in (1) implies the marginal distribution of \mathbf{X}

$$\mathbf{X} \sim \mathcal{N}(\mathbf{0}, \boldsymbol{\Sigma}(\boldsymbol{\theta})), \quad (2)$$

where $\boldsymbol{\Sigma}(\boldsymbol{\theta}) = \boldsymbol{\Lambda}\boldsymbol{\Phi}\boldsymbol{\Lambda}' + \boldsymbol{\Omega}$. Without further constraints, the parameters in (2) are not identifiable due to rotational indeterminacy. That is, two sets of parameters $\boldsymbol{\theta}$ and $\tilde{\boldsymbol{\theta}} = (\tilde{\boldsymbol{\Lambda}}, \tilde{\boldsymbol{\Phi}}, \tilde{\boldsymbol{\Omega}})$ give the same distribution for \mathbf{X} if $\boldsymbol{\Lambda}\boldsymbol{\Phi}\boldsymbol{\Lambda}' = \tilde{\boldsymbol{\Lambda}}\tilde{\boldsymbol{\Phi}}\tilde{\boldsymbol{\Lambda}}'$ and $\boldsymbol{\Omega} = \tilde{\boldsymbol{\Omega}}$. Note that the normality assumptions above are not essential. They are adopted for the ease of writing, and the development in the current paper does not rely on these normality assumptions. Throughout this paper, we assume that the number of factors K is known.

An oblique rotation method is a two-step procedure. In the first step, one obtains an estimate of the model parameters, under the constraints that $\boldsymbol{\Phi} = \mathbf{I}$ and other arbitrary but mathematically convenient constraints that fix the rotational indeterminacy. Note that due to the rotational indeterminacy, one can always constrain $\boldsymbol{\Phi} = \mathbf{I}$ and absorb the dependence between the factors into the loading matrix $\boldsymbol{\Lambda}$. The estimate can be obtained by any reasonable estimator for factor analysis, such as the least-square (Jöreskog & Goldberger, 1972), weighted-least-square (Browne, 1984), and maximum likelihood estimators (Jöreskog, 1967). We denote this estimator by $\hat{\boldsymbol{\theta}} = (\hat{\boldsymbol{\Lambda}}, \mathbf{I}, \hat{\boldsymbol{\Omega}})$. In the second step, one finds an oblique rotation matrix

$\hat{\mathbf{T}}$, such that the rotated loading matrix $\hat{\Lambda} = \hat{\mathbf{A}}\hat{\mathbf{T}}'^{-1}$ minimises a certain loss function Q that measures the sparsity level of a loading matrix. The functional form of Q will be proposed in the sequel. Here, an oblique rotation matrix \mathbf{T} satisfies that \mathbf{T} is invertible and $(\mathbf{T}'\mathbf{T})_{kk} = 1, k = 1, \dots, K$. Consequently, any rotated solution $(\hat{\mathbf{A}}\hat{\mathbf{T}}'^{-1}, \mathbf{T}'\mathbf{T}, \hat{\Omega})$ is still in the parameter space and gives the same distribution for X . More precisely, we let

$$\mathcal{M} = \{\mathbf{T} \in \mathbb{R}^{K \times K} : \text{rank}(\mathbf{T}) = K, (\mathbf{T}'\mathbf{T})_{kk} = 1, k = 1, \dots, K\} \quad (3)$$

be the space for oblique rotation matrices, where $\text{rank}(\cdot)$ gives the rank of a matrix. Then the oblique rotation problem involves solving the optimisation

$$\hat{\mathbf{T}} \in \arg \min_{\mathbf{T} \in \mathcal{M}} Q(\hat{\mathbf{A}}\mathbf{T}'^{-1}), \quad (4)$$

and the rotated solution is given by $(\hat{\mathbf{A}}\hat{\mathbf{T}}'^{-1}, \hat{\mathbf{T}}'\hat{\mathbf{T}}, \hat{\Omega})$. Equivalently, the rotated loading matrix $\hat{\Lambda}$ satisfies

$$(\hat{\Lambda}, \hat{\Phi}) \in \arg \min_{\Lambda, \Phi} Q(\Lambda), \text{ such that } \Lambda\Phi\Lambda' = \hat{\Lambda}\hat{\Lambda}'. \quad (5)$$

As explained in Remark 1, the minimiser of (4) or equivalently that of (5) is not unique.

Remark 1. Let \mathcal{D}_1 be the set of all $K \times K$ permutation matrices and \mathcal{D}_2 be the set of all $K \times K$ sign flip matrices. For any $\mathbf{D}_1 \in \mathcal{D}_1, \mathbf{D}_2 \in \mathcal{D}_2$, and $K \times K$ matrix \mathbf{T} , $\mathbf{T}\mathbf{D}_1$ is a matrix whose columns are a permutation of those of \mathbf{T} and, $\mathbf{T}\mathbf{D}_2$ is a matrix whose k th column is either the same as the k th column of \mathbf{T} or the k th column of \mathbf{T} multiplied by -1 . Let $\hat{\mathbf{T}}$ be one solution to the optimisation problem (4). It is easy to check that $\hat{\mathbf{T}}\mathbf{D}_1\mathbf{D}_2$ also minimises the objective function (4), for any $\mathbf{D}_1 \in \mathcal{D}_1$ and $\mathbf{D}_2 \in \mathcal{D}_2$. The resulting loading matrix is equivalent to $\hat{\Lambda}$ up to a column permutation and column sign flips.

We conclude the problem setup with two remarks.

Remark 2. The rotation problem not only applies to the linear factor model, but also other settings, such as item factor analysis (Chen et al., 2021; Chen et al., 2019; Reckase, 2009) and machine learning models (Rohe & Zeng, 2022).

Remark 3. Although the current paper focuses on oblique rotations, we note that the proposed criteria can be easily extended to orthogonal rotation, as the latter can be viewed as a special case of the former when Φ is fixed to be an identity matrix. That is, given a loss function Q , orthogonal rotation solves the problem

$$\min_{\Lambda} Q(\Lambda), \text{ such that } \Lambda\Lambda' = \hat{\Lambda}\hat{\Lambda}'.$$

2.2 Proposed Rotation Criteria

Jennrich (2004, 2006) proposed a family of monotone concave CLFs for the choice of Q in (4), taking the form

$$Q(\Lambda) = \sum_{j=1}^J \sum_{k=1}^K h(|\lambda_{jk}|), \quad (6)$$

where $\Lambda = (\lambda_{jk})_{J \times K}$ and h is a concave and monotone increasing function that maps from $[0, \infty)$ to $[0, \infty)$. This family of loss functions is appealing for several reasons. First, a CLF takes a simple form that does not

involve products of loadings and their higher-order polynomial terms. Second, the monotone concave CLFs have desired properties. In particular, Jennrich (2006) proved that a monotone concave CLF is minimized by loadings with perfect simple structure when such loadings exist. Third, simulation studies in Jennrich (2004, 2006) showed that these loss functions tend to outperform traditional rotation methods, e.g. (promax, simplimax, quartimin and geomin) when the true loading matrix is sparse.

Two examples of h are given in Jennrich (2004, 2006), including the linear CLF where $h(|\lambda|) = |\lambda|$ and the basic CLF where $h(|\lambda|) = 1 - \exp(-|\lambda|)$. However, there does not exist a full spectrum of monotone concave CLFs for dealing with true loading matrices with different sparsity levels. To fill this gap, we propose a general family of monotone concave CLFs that are named the L^p CLFs. More specifically, for each value of $p \in (0, 1]$, the loss function takes the form

$$Q_p(\mathbf{\Lambda}) = \sum_{j=1}^J \sum_{k=1}^K |\lambda_{jk}|^p, \quad (7)$$

Proposition 1 below shows that this choice of h yields a monotone concave CLF.

Proposition 1. *The absolute value function $h(x) = |x|^p$, $p \in (0, 1]$ is monotonically increasing and concave on the interval $[0, \infty)$.*

Under very mild regularity conditions, any L^p CLF is uniquely minimized by a loading matrix of perfect simple structure when such loading matrix exist, where we say the minimiser is unique when all the minimisers of the loss function are equivalent up to column permutation and sign flip transformations (see Remark 1 for these transformations). We summarise this result in Proposition 2 below. This result improves Theorem 1 of Jennrich (2006), as the uniqueness of the perfect simple structure is not established in Jennrich (2006) for the L^1 -criterion.

Proposition 2. *Suppose that the true loading matrix $\mathbf{\Lambda}^*$ has perfect simple structure, in the sense that each row has at most one nonzero entry. Further suppose that $\mathbf{\Lambda}^*$ is of full column rank, i.e., $\text{rank}(\mathbf{\Lambda}^*) = K$. Then for any oblique rotation matrix $\mathbf{T} \in \mathcal{M}$,*

$$Q_p(\mathbf{\Lambda}^* \mathbf{T}'^{-1}) \geq Q_p(\mathbf{\Lambda}^*),$$

where the two sides are equal if and only if $\mathbf{T}'^{-1} = \mathbf{D}_1 \mathbf{D}_2$ for $\mathbf{D}_1 \in \mathcal{D}_1$ and $\mathbf{D}_2 \in \mathcal{D}_2$.

Why do we need the loss functions with $p < 1$, given that the choice of $p = 1$ is already available in Jennrich (2004, 2006)? This is because different L^p CLFs were found to behave differently when the true loading matrix does not have a perfect simple structure but still contains many zero loadings. Such a loading structure is more likely to be recovered by an L^p CLF when $p < 1$ than the L^1 CLF. In what follows, we elaborate on this point. Let $\mathbf{\Lambda}^*$ be the true sparse loading matrix and $\mathbf{\Phi}^*$ be the corresponding covariance matrix for the factors. For the true loading matrix $\mathbf{\Lambda}^*$ to be recovered by an L^p CLF, a minimum requirement is that

$$Q_p(\mathbf{\Lambda}^*) = \min_{\mathbf{\Lambda}} Q_p(\mathbf{\Lambda}), \text{ such that there exists } \mathbf{\Phi} \succ 0, \phi_{kk} = 1, k = 1, \dots, K, \mathbf{\Lambda}^* \mathbf{\Phi}^* \mathbf{\Lambda}^{*'} = \mathbf{\Lambda} \mathbf{\Phi} \mathbf{\Lambda}'. \quad (8)$$

In other words, $\mathbf{\Lambda}^*$ needs to be a stationary point of Q_p . Figure 1 gives the plots for $|x|^p$ with different choices of p and their derivatives when $x > 0$. We note that when $p < 1$ the derivative of $|x|^p$ converges to infinity as x approaching zero. The smaller the value of p , the faster the convergence speed is. On the other

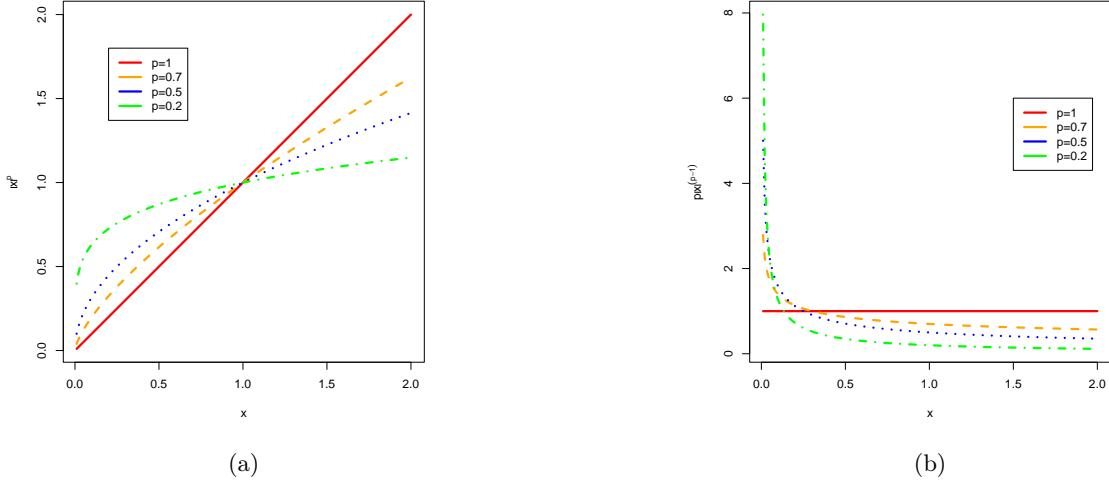


Figure 1: Panel (a): Plots of $|x|^p$, for different choices of p . Panel (b): Plots of the derivative of $|x|^p$, for different choices of p .

hand, when $p = 1$, the derivative of $|x|$ takes the value one for any $x > 0$. Therefore, when $\mathbf{\Lambda}^*$ is sparse but does not have a perfect simple structure, it is more likely to be a stationary point of Q_p for $p < 1$ than Q_1 . We illustrate this point by a numerical example, where $\mathbf{\Lambda}^*$ is given below and $\mathbf{\Phi}^*$ is set to be an identity matrix

$$\mathbf{\Lambda}^{*'} = \begin{pmatrix} 1.20 & 0 & 0.15 & 0 & 0.25 & 1.05 & 0.18 \\ 0 & 0.27 & 0 & 1.04 & 0.15 & 1.29 & 0.11 \end{pmatrix}.$$

Figure 2 shows the contour plots of $Q_p(\mathbf{\Lambda})$ for $\mathbf{\Lambda}$ satisfying the constraints in (8), with $p = 0.5$ and 1, respectively. It is not difficult to show that when $K = 2$, $\mathbf{\Lambda}$ satisfying the constraints in (8) has two degrees of freedoms, which are parameterised by (θ_1, θ_2) in each plot. The point $(0, 0)$, which is indicated by a black cross, corresponds to $\mathbf{\Lambda} = \mathbf{\Lambda}^*$, and the point indicated by a red point corresponds to the $\mathbf{\Lambda}$ matrix such that $Q_p(\mathbf{\Lambda})$ is minimised. As we can see, when $p = 0.5$, the loss function is minimised by $\mathbf{\Lambda}^*$. On the other hand, when $p = 1$, the minimiser of the loss function does not contain as many zeros as $\mathbf{\Lambda}^*$.

Finally, we remark that due to the singularity of L^p function near zero when $p < 1$, the optimisation for Q_p tends to be more challenging with a smaller value of p . This is also reflected by the contour plots in Figure 2, where we see $Q_{0.5}$ is very non-convex, even around the minimiser. On the other hand, Q_1 seems locally convex near the minimiser. Therefore, although the L^p -rotation with $p < 1$ may be better at recovering sparse loading matrices, its computation is more challenging.

2.3 Connection with regularised estimation

The proposed rotation criteria have a close connection with regularised estimators for EFA. In what follows, we establish this connection. Recall that the proposed procedure relies on an initial estimator of the loading matrix for which $\mathbf{\Phi}$ is constrained to be an identity matrix. We further require it to be an M -estimator, obtained by minimising a certain loss function, denoted by $L(\mathbf{\Sigma}(\boldsymbol{\theta}))$. Note that all the popular EFA estimators are all M -estimators. For instance, when the maximum likelihood estimator is used, then the loss function

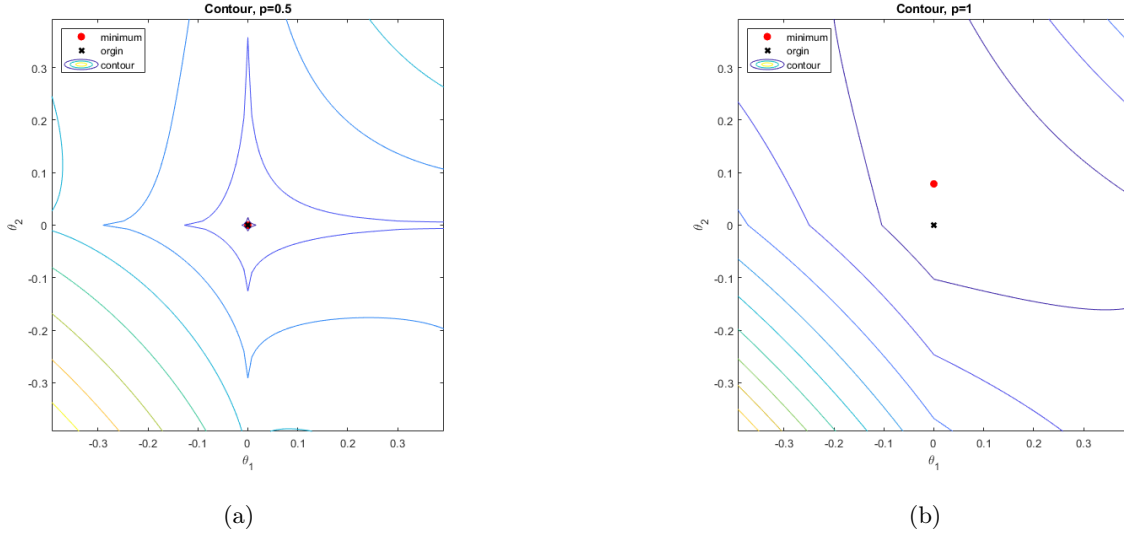


Figure 2: Plots of contours of $|\mathbf{\Lambda}^* \mathbf{T}^{-1}|^p$, where $\mathbf{T} = [\cos(\theta_1), \sin(\theta_2); \sin(\theta_1), \cos(\theta_2)]$. Panel (a): $p = 0.5$. Panel (b): $p = 1$.

to be minimised is

$$L(\mathbf{\Sigma}(\boldsymbol{\theta})) = \log \det(\mathbf{\Sigma}(\boldsymbol{\theta})) + \text{tr}(\mathbf{\Sigma}(\boldsymbol{\theta})^{-1} \mathbf{S}),$$

where $\mathbf{S} = (\sum_{i=1}^N \mathbf{x}_i \mathbf{x}_i^\top) / N$ is the sample covariance matrix.

Now we introduce an L^p regularised estimator based on the loss function $L(\mathbf{\Sigma}(\boldsymbol{\theta}))$ in the form

$$\hat{\boldsymbol{\theta}}_{\gamma,p} \in \arg \min_{\boldsymbol{\theta}} L(\mathbf{\Sigma}(\boldsymbol{\theta})) + \gamma \sum_{j=1}^J \sum_{k=1}^K |\lambda_{jk}|^p, \quad (9)$$

where $\gamma > 0$ is a tuning parameter and the covariance matrix $\mathbf{\Phi}$ is estimated rather than constrained to be an identity matrix. We note that the minimiser of (9) is also not unique due to column permutation and sign flips similar to the non-uniqueness of optimisation (4). We denote the set of minimisers as

$$\hat{\mathcal{C}}_{\gamma,p} = \arg \min_{\boldsymbol{\theta}} L(\mathbf{\Sigma}(\boldsymbol{\theta})) + \gamma \sum_{j=1}^J \sum_{k=1}^K |\lambda_{jk}|^p.$$

Note that the regularisation term takes the same form as the L^p CLF. It is used to impose sparsity on the estimate of the loading matrix. When $p = 1$, it becomes a LASSO regularised estimator that has been considered in for example Choi et al. (2010), Hirose and Yamamoto (2014, 2015), Jin et al. (2018) and Geminiani et al. (2021). The regularised estimator (9) is similar in spirit to L^p -regularised regression (Lai & Wang, 2011; Mazumder et al., 2011; Zheng et al., 2017), where the L^p regularisation with $p < 1$ has been shown to better recover sparse signals under high-dimensional linear regression settings while computationally more challenging (Zheng et al., 2017).

As summarised in Proposition 3 below, the proposed L^p rotation solution can be viewed as a limiting case of the L^p -regularised estimator when the tuning parameter γ converges to zero.

Proposition 3. *Consider a fixed $p \in (0, 1]$ and a fixed dataset. Suppose that for any sufficiently small $\gamma > 0$, $\hat{\mathcal{C}}_{\gamma,p}$ only contains $n = 2^K K!$ elements that are equivalent up to column permutation and sign flips*

of the loading matrix, where $K!$ denotes K factorial that counts the number of all possible permutations and 2^K gives the total number of sign flip transformations. Furthermore, assume that for any sufficiently small $\gamma > 0$, one can label the elements of $\hat{\mathbf{C}}_{\gamma,p}$, denoted by $\hat{\boldsymbol{\theta}}_{\gamma,p}^{(i)}$, $i = 1, \dots, n$, such that there exists a sufficiently small constant $\delta > 0$, $\hat{\boldsymbol{\theta}}_{\gamma,p}^{(i)}$ is a continuous and bounded function of γ in $(0, \delta)$, for each i . Then the limit

$$\hat{\boldsymbol{\theta}}_{0,p}^{(i)} = (\hat{\boldsymbol{\Lambda}}_{0,p}^{(i)}, \hat{\boldsymbol{\Phi}}_{0,p}^{(i)}, \hat{\boldsymbol{\Omega}}_{0,p}^{(i)}) = \lim_{\gamma \rightarrow 0} \hat{\boldsymbol{\theta}}_{\gamma,p}^{(i)}$$

exists, and $\hat{\boldsymbol{\theta}}_{0,p}^{(i)}$ satisfies that $(\hat{\boldsymbol{\Lambda}}_{0,p}^{(i)}, \hat{\boldsymbol{\Phi}}_{0,p}^{(i)})$ solves the optimisation problem (5) and $\hat{\boldsymbol{\Omega}}_{0,p}^{(i)} = \hat{\boldsymbol{\Omega}}$, where $\hat{\boldsymbol{\theta}} = (\hat{\boldsymbol{\Lambda}}, \mathbf{I}, \hat{\boldsymbol{\Omega}})$ minimises the loss function $L(\boldsymbol{\Sigma}(\boldsymbol{\theta}))$.

We now discuss the implications of this connection. First, if we have a numerical solver for the regularised estimator (9), then one can obtain an approximate solution to the L^p -rotation problem (5) by using a sufficiently small tuning parameter γ . Second, thanks to this connection, the choice between regularised estimation and rotation becomes the choice of the tuning parameter in regularised estimation. Note that the tuning parameter γ corresponds to a bias-variance trade-off in estimating the model parameters $\boldsymbol{\theta}$. As γ increases, the bias of the regularised estimator increases and the variance decreases. In applications where the sample size is large relative to the number of model parameters, the optimal choice of the tuning parameter is often close to zero. In that case, it is a good idea to use the rotation method, as the regularised estimator under the optimal tuning parameter may not be substantially more accurate than the rotation solution and searching for the optimal tuning parameter can be computationally costly. The computation of these methods will be discussed in Section 4.

3 Statistical Inference and Asymptotic Theory

3.1 Estimation Consistency

We establish the statistical consistency of the proposed estimator based on the L^p rotation. Suppose the true parameter set that we aim to recover is $(\boldsymbol{\Lambda}^*, \boldsymbol{\Phi}^*, \boldsymbol{\Omega}^*)$, where the true loading matrix $\boldsymbol{\Lambda}^*$ is sparse. To emphasise the dependence on the sample size, we attach the sample size N as a subscript to the initial estimator in the first step of the rotation method; that is, $\hat{\boldsymbol{\theta}}_N = (\hat{\boldsymbol{\Lambda}}_N, \mathbf{I}, \hat{\boldsymbol{\Omega}}_N)$. We require the initial estimator to be consistent, in the sense that

- C1. $\hat{\boldsymbol{\Lambda}}_N \hat{\boldsymbol{\Lambda}}_N' \xrightarrow{pT} \boldsymbol{\Lambda}^* \boldsymbol{\Phi}^* \boldsymbol{\Lambda}^{*'} and $\hat{\boldsymbol{\Omega}}_N \xrightarrow{pT} \boldsymbol{\Omega}^*$, where the notation " \xrightarrow{pT} " denotes convergence in probability.$

This requirement easily holds when the linear factor model is correctly specified and the loss function $L(\boldsymbol{\Sigma}(\boldsymbol{\theta}))$ is reasonable (e.g., the negative log-likelihood). In addition, we require that the EFA model is truly a K -dimensional model, in the sense that condition C2 holds.

- C2. $rank(\boldsymbol{\Lambda}^* \boldsymbol{\Phi}^* \boldsymbol{\Lambda}^{*'}) = K$.

For the the L^p rotation estimator to be consistent, for a specific value of $p \in (0, 1]$, we further require that the true loading matrix uniquely minimises the L^p CLF, in the sense of condition C3 below.

- C3. $(\boldsymbol{\Lambda}^*, \boldsymbol{\Phi}^*) \in \arg \min_{\boldsymbol{\Lambda}, \boldsymbol{\Phi}} Q_p(\boldsymbol{\Lambda})$ such that $\boldsymbol{\Lambda} \boldsymbol{\Phi} \boldsymbol{\Lambda}' = \boldsymbol{\Lambda}^* \boldsymbol{\Phi}^* \boldsymbol{\Lambda}^{*}$. In addition, for any other $(\boldsymbol{\Lambda}^\dagger, \boldsymbol{\Phi}^\dagger) \in \arg \min_{\boldsymbol{\Lambda}, \boldsymbol{\Phi}} Q_p(\boldsymbol{\Lambda})$ such that $\boldsymbol{\Lambda} \boldsymbol{\Phi} \boldsymbol{\Lambda}' = \boldsymbol{\Lambda}^* \boldsymbol{\Phi}^* \boldsymbol{\Lambda}^{*}$, there exist $\mathbf{D} \in \mathcal{D}_1$ and $\tilde{\mathbf{D}} \in \mathcal{D}_2$, such that $\boldsymbol{\Lambda}^\dagger \mathbf{D} \tilde{\mathbf{D}} = \boldsymbol{\Lambda}^*$ and $\tilde{\mathbf{D}}^{-1} \mathbf{D}^{-1} \boldsymbol{\Phi}^\dagger (\mathbf{D}^{-1})' (\tilde{\mathbf{D}}^{-1})' = \boldsymbol{\Phi}^*$. Recall that \mathcal{D}_1 and \mathcal{D}_2 are the sets of column permutation and sign flip transformations, respectively, which are given in Remark 1.

Condition C3 tends to hold when the true loading matrix contains many zeros, as the L^p loss function is a good approximation to the L^0 function that counts the number of non-zero elements. In particular, according to Proposition 2, condition C3 is guaranteed to hold when $\mathbf{\Lambda}^*$ has a perfect simple structure, i.e., if it has at most one nonzero loading in each row. As discussed in Section 2.2, this condition is more likely to hold for a smaller value of p , when there are cross loadings. Conditions C1 through C3 guarantee the estimation consistency of the L^p rotation estimator, up to column permutation and sign flips. This result is summarised in Theorem 1 below.

Theorem 1. *Suppose that for a given $p \in (0, 1]$ conditions C1 through C3 hold. Then there exist $\mathbf{D}_N \in \mathcal{D}_1$ and $\tilde{\mathbf{D}}_N \in \mathcal{D}_2$, such that $\hat{\mathbf{\Lambda}}_{N,p} \mathbf{D}_N \tilde{\mathbf{D}}_N \xrightarrow{pr} \mathbf{\Lambda}^*$ and $\tilde{\mathbf{D}}_N^{-1} \mathbf{D}_N^{-1} \hat{\mathbf{\Phi}}_{N,p} (\mathbf{D}_N^{-1})' (\tilde{\mathbf{D}}_N^{-1})' \xrightarrow{pr} \mathbf{\Phi}^*$, where*

$$(\hat{\mathbf{\Lambda}}_{N,p}, \hat{\mathbf{\Phi}}_{N,p}) \in \arg \min_{\mathbf{\Lambda}, \mathbf{\Phi}} Q_p(\mathbf{\Lambda}), \text{ such that } \mathbf{\Lambda} \mathbf{\Phi} \mathbf{\Lambda}' = \hat{\mathbf{\Lambda}}_N \hat{\mathbf{\Lambda}}_N'.$$

3.2 Model Selection

The interpretation of the factors relies on the sign pattern of the loading matrix, so that each factor can be interpreted based on the associated manifest variables and their directions (positive or negative associations). Learning this sign pattern is a model selection problem. A regularised estimator may seem advantageous as it yields simultaneous parameter estimation and model selection. We note that, however, model selection can be easily achieved with a rotation method, using a Hard-Thresholding (HT) procedure. Similar HT procedures have been proven successful in the model selection for linear regression models (Meinshausen & Yu, 2009).

More precisely, let $\mathbf{\Gamma}^* = \left(\text{sgn}(\lambda_{jk}^*) \right)_{J \times K}$ denote the true sign pattern of $\mathbf{\Lambda}^*$, where $\text{sgn}(x)$ returns the sign of a scalar satisfying that

$$\text{sgn}(x) = \begin{cases} 1 & \text{if } x > 0, \\ 0 & \text{if } x = 0, \\ -1 & \text{if } x < 0. \end{cases}$$

Given the L^p rotation estimator $\hat{\mathbf{\Lambda}}_{N,p} = \left(\hat{\lambda}_{jk}^{(N,p)} \right)_{J \times K}$, the HT procedure estimates the pattern of $\mathbf{\Gamma}^*$ by $\hat{\mathbf{\Gamma}}_{N,p} = \left(\text{sgn}(\hat{\lambda}_{jk}^{(N,p)}) \times 1_{\{|\hat{\lambda}_{jk}^{(N,p)}| > c\}} \right)_{J \times K}$, where $c > 0$ is a pre-specified threshold. If the threshold c is chosen properly, then $\hat{\mathbf{\Gamma}}_{N,p}$ consistently estimates $\mathbf{\Gamma}^*$. We state this result in Theorem 2 below.

C4. The threshold c lies in the interval $(0, c_0)$, where $c_0 = \min\{|\lambda_{jk}^*| : \lambda_{jk}^* \neq 0\}$.

Theorem 2. *Suppose that for a given $p \in (0, 1]$ conditions C1 through C4 hold. Then there exist $\mathbf{D}_N \in \mathcal{D}_1$ and $\tilde{\mathbf{D}}_N \in \mathcal{D}_2$, such that the probability $P(\hat{\mathbf{\Gamma}}_{N,p} \mathbf{D}_N \tilde{\mathbf{D}}_N = \mathbf{\Gamma}^*)$ converges to 1 as the sample size N goes to infinity.*

In practice, the value of c_0 is unknown and thus cannot be used for choosing the threshold c . Instead, we choose c based on the Bayesian Information Criterion (BIC; Schwarz, 1978). The steps of this procedure are summarised in Algorithm 1 below, where the notation is simplified for the ease of exposition.

When the candidate values of c are chosen properly (i.e., \mathcal{C} includes values that are below c_0), then Theorem 2 implies that with probability tending to one, the true model will be in the candidate models. Together with the consistency of BIC for parametric models (Shao, 1997; Vrieze, 2012), the true non-zero pattern can be consistently recovered.

Algorithm 1 Hard-thresholding for model selection based on L^p rotation

Input: A sequence of candidate thresholds \mathcal{C} , observed data, and the rotated loading matrix $\hat{\mathbf{\Lambda}} = (\hat{\lambda}_{jk})_{J \times K}$ given by the L^p CLF criterion.

For each value of $c \in \mathcal{C}$, we perform the following two steps:

Step 1: Obtain the corresponding selected loading structure $\hat{\mathbf{\Gamma}}_c = \left(\text{sgn}(\hat{\lambda}_{jk}) \times 1_{\{|\hat{\lambda}_{jk}| > c\}} \right)_{J \times K}$.

Step 2: Fit a Confirmatory Factor Analysis (CFA) model based on $\hat{\mathbf{\Gamma}}_c$ using the maximum likelihood estimator, in which the (i, j) th loading parameter satisfies the sign constraint implied by the corresponding entry of $\hat{\mathbf{\Gamma}}_c$. Calculate the BIC value for this CFA model, denoted by BIC_c .

Obtain $\hat{c} = \arg \min_{c \in \mathcal{C}} \text{BIC}_c$.

Output: The selected sign pattern $\hat{\mathbf{\Gamma}}_{\hat{c}}$.

3.3 Confidence Intervals

Often, we are not only interested in the point estimate of the underlying sparse loading matrix, but also in quantifying its uncertainty. Uncertainty quantification is typically achieved by constructing confidence intervals for the loadings of the rotated solution. Traditionally, this is achieved by establishing the asymptotic normality of the rotated loading matrix using the delta method, which involves calculating the partial derivatives of a rotation algorithm using implicit differentiation (Jennrich, 1973). Unfortunately, this procedure is no longer suitable, if the true loading matrix is sparse and the loss function is not differentiable with respect to the zero loadings.

Motivated by a simple while well-performing post-selection inference procedure in regression analysis (Zhao et al., 2021), we propose a procedure for constructing confidence intervals for individual loading parameters of the rotated solution. More precisely, this procedure runs a loop over all the manifest variables, $j = 1, \dots, J$. Each time, the procedure obtains the confidence intervals for the loading parameters of manifest variable j , by fitting a CFA model whose the loading structure is determined by the selected sign pattern of the rest $J - 1$ manifest variables. More precisely, the loading parameters of the CFA model satisfy the sign constraints imposed by the selected sign pattern $\hat{\mathbf{\Gamma}}_{\hat{c}}$ from Algorithm 1, for all the items except for j . No constraint is imposed on the loading parameters of item j . Confidence intervals for the loading parameters of item j are obtained based on the asymptotic normality of the estimator for this CFA model. We summarise this procedure in Algorithm 2 below.

Algorithm 2 Post-selection confidence intervals

Input: The selected sign pattern $\hat{\mathbf{\Gamma}} = (\hat{\gamma}_{jk})_{J \times K}$, observed data, and significance level $\alpha \in (0, 1)$.

For each manifest variable $s = 1, \dots, J$, we perform the following two steps.

Step 1: Obtain a CFA model whose loadings λ_{jk} satisfy the constraints that $\text{sgn}(\lambda_{jk}) = \hat{\gamma}_{jk}$ for all $j \neq s$.

Step 2: Fit the CFA model and obtain the $(1 - \alpha)$ -confidence intervals for parameters $\lambda_{s1}, \dots, \lambda_{sK}$ using a standard inference procedure for CFA (e.g., based on the maximum likelihood estimator). We denote these confidence intervals by (l_{sk}, u_{sk}) . If the CFA model in **Step 1** is not identifiable, we let the confidence intervals to be $(-\infty, \infty)$.

Output: Confidence intervals (l_{sk}, u_{sk}) , $s = 1, \dots, J, k = 1, \dots, K$.

In what follows, we establish the consistency of confidence intervals given by Algorithm 2. To emphasize that the statistics in Algorithm 2 depend on the sample size N , we attach N as a subscript or superscript when describing this consistency result. We require the following conditions.

C5. The selected sign pattern $\hat{\Gamma}_N$ is consistent. That is, there exist $\mathbf{D}_N \in \mathcal{D}_1$ and $\tilde{\mathbf{D}}_N \in \mathcal{D}_2$, such that the probability $P(\hat{\Gamma}_{N,p} \mathbf{D}_N \tilde{\mathbf{D}}_N = \Gamma^*)$ converges to 1 as the sample size N goes to infinity.

Thanks to the consistency of BIC selection and when the candidate thresholds are chosen properly, condition C5 holds if $\hat{\Gamma}_N$ is obtained by Algorithm 1.

C6. For each manifest variable $s = 1, \dots, J$, the CFA model whose loading parameters satisfy $\text{sgn}(\lambda_{jk}) = \text{sgn}(\lambda_{jk}^*)$ for all $j \neq s$ is identifiable, and using the same procedure in Step 2 of Algorithm 2 leads to consistent confidence intervals for $\lambda_{s1}, \dots, \lambda_{sK}$. That is, let $(l_{sk}^{*(N)}, u_{sk}^{*(N)})$ be the resulting confidence interval for λ_{sk} , then $P(\lambda_{sk}^* \in (l_{sk}^{*(N)}, u_{sk}^{*(N)}))$ converges to $1 - \alpha$, as the sample size N goes to infinity.

Note that C6 is a condition imposed on the sign pattern of the true loading matrix. It essentially requires that the factors can be identified by the sign pattern of any $(J-1)$ -subset of the manifest variables. Given an identified CFA model, the consistent confidence intervals can be easily constructed based on the asymptotic normality of any reasonable estimator of the CFA model, e.g., the maximum likelihood estimator. Under conditions C5 and C6, the following theorem holds.

Theorem 3. *Suppose that conditions C5 and C6 hold for the selected sign pattern $\hat{\Gamma}_N$ and the true model, where $\mathbf{D}_N \in \mathcal{D}_1$ and $\tilde{\mathbf{D}}_N \in \mathcal{D}_2$ are from condition C5. Suppose we input $\hat{\Gamma}_N$, observed data from the true model, and significance level α into the true model, and obtain output $(l_{sk}^{(N)}, u_{sk}^{(N)})$, $s = 1, \dots, J, k = 1, \dots, K$. Then we have $P(\lambda_{sk}^{*(N)} \in (l_{sk}^{(N)}, u_{sk}^{(N)}))$ converges to $1 - \alpha$, for all $s = 1, \dots, J, k = 1, \dots, K$, where $\lambda_{sk}^{*(N)}$ are entries of $\Lambda^{*(N)} = \Lambda^* \tilde{\mathbf{D}}_N^{-1} \mathbf{D}_N^{-1}$. Note that $\Lambda^{*(N)}$ is equivalent to Λ^* up to column permutation and sign flips.*

We remark that under the conditions of Theorem 3, all the CFA models fitted in Step 2 of Algorithm 2 should be identifiable for sufficiently large N . However, in practice, it may happen that some CFA models are not identifiable, either due to that the sample size is not large enough or that the regularity conditions C5 or C6 does not hold. In that case, we set the corresponding confidence intervals to be $(-\infty, \infty)$ as a conservative choice.

4 Computation

4.1 Proposed IRGP Algorithm

We now discuss the computation for the proposed rotation. Recall that we aim to solve the optimisation problem

$$\hat{\mathbf{T}} \in \arg \min_{\mathbf{T} \in \mathcal{M}} Q_p(\hat{\mathbf{A}} \mathbf{T}'^{-1}),$$

where Q_p is the L^p CLF defined in (7). Note that this objective function is not differentiable when $\hat{\mathbf{A}} \mathbf{T}'^{-1}$ has zero elements, as the L^p function is not smooth at zero. Consequently, standard numerical solvers fail, especially when the true solution is approximately sparse. To solve this optimisation problem, we develop an Iteratively Reweighted Gradient Projection (IRGP) algorithm that combines the iteratively reweighted least

square algorithm (Ba et al., 2013; Daubechies et al., 2010) and the gradient projection algorithm (Jennrich, 2002).

Similar to Jennrich (2006), the IRGP algorithm also solves a smooth approximation to the objective function $Q_p(\hat{\mathbf{A}}\mathbf{T}'^{-1})$. That is, we introduce a sufficiently small constant $\epsilon > 0$, and approximate the objective function by $Q_{p,\epsilon}(\hat{\mathbf{A}}\mathbf{T}'^{-1})$, where

$$Q_{p,\epsilon}(\mathbf{\Lambda}) = \sum_{j=1}^J \sum_{k=1}^K (\epsilon^2 + \lambda_{jk}^2)^{\frac{p}{2}}.$$

As discussed in the sequel, the ϵ is introduced to robustify the computation. The IRGP algorithm alternates between two steps – (1) function approximation step and (2) Projected Gradient Descent (PGD) step. More precisely, let T_t be the parameter value at the t th iteration.

The function approximation step involves approximating the objective function by

$$G_t(\mathbf{T}) = \sum_{j=1}^J \sum_{k=1}^K w_{jk}^{(t)} \left((\hat{\mathbf{A}}\mathbf{T}'^{-1})_{jk} \right)^2, \quad (10)$$

where the weights $w_{jk}^{(t)}$ are given by

$$w_{jk}^{(t)} = \frac{1}{((\hat{\mathbf{A}}(\mathbf{T}'_t)^{-1})_{jk}^2 + \epsilon^2)^{\frac{p}{2}}}.$$

Here $\epsilon > 0$ is a pre-specified parameter that is chosen sufficiently small. We provide some remarks about this approximation. First, the small tuning parameter is chosen to stabilise the algorithm when certain $(\hat{\mathbf{A}}(\mathbf{T}'_t)^{-1})_{jk}$ s are close to zero. Without ϵ , the weight $w_{jk}^{(t)}$ can become vary large, resulting in an unstable PGD step. Second, supposing that $(\hat{\mathbf{A}}(\mathbf{T}'_t)^{-1})_{jk} \neq 0$ for all j and k , then $G_t(\mathbf{T}_t) \approx Q_p(\hat{\mathbf{A}}(\mathbf{T}'_t)^{-1})$ when ϵ is sufficiently small, i.e., the function approximation and the objective function value are close to each other at the current parameter value. Lastly, this approximation is similar to the E-step of the Expectation-Maximisation algorithm (Dempster et al., 1977); see Ba et al. (2013) for this correspondence.

The PGD step involves updating the parameter value based on the $G_t(\mathbf{T})$ via projected gradient descent. This step is similar to the update in each iteration of the gradient projection algorithm for oblique rotations (Jennrich, 2002). PGD can be performed to $G_t(\mathbf{T})$, as this function approximation is smooth in \mathbf{T} . More precisely, we define a projection operator as

$$\text{Proj}(\mathbf{T}) = \mathbf{T}(\text{diag}(\mathbf{T}'\mathbf{T}))^{-\frac{1}{2}}, \quad (11)$$

where $(\text{diag}(\mathbf{T}'\mathbf{T}))^{-\frac{1}{2}}$ is a diagonal matrix whose i th diagonal entry is given by $1/\sqrt{(\mathbf{T}'\mathbf{T})_{ii}}$. This operator projects any invertible matrix into the space of oblique matrices \mathcal{M} . The PGD update is given by

$$\mathbf{T}_{t+1} = \text{Proj}(\mathbf{T}_t - \alpha \nabla G_t(\mathbf{T})), \quad (12)$$

where $\alpha > 0$ is a step size chosen by line search and $\nabla G_t(\mathbf{T})$ is a $K \times K$ matrix whose (i, j) th entry is the partial derivative of $G_t(\mathbf{T})$ with respect to (i, j) th entry of \mathbf{T} . We summarise the IRGP algorithm below.

Under reasonable regularity conditions (Ba et al., 2013), every limit point of $\{\mathbf{T}_t\}_{t=1}^{\infty}$ will be a stationary point of the approximated objective function $Q_{p,\epsilon}(\hat{\mathbf{A}}\mathbf{T}'^{-1})$. In addition, the algorithm has local linear

Algorithm 3 IRGP algorithm for L^p rotation

Input: The initial loading matrix estimate $\hat{\mathbf{A}}$, parameter $\epsilon > 0$, and an initial value \mathbf{T}_0 .

For iterations $t = 0, 1, 2, \dots$, we iterate between the following two steps:

Step 1: Construct $G_t(\mathbf{T})$ using equation (10).

Step 2: Obtain \mathbf{T}_{t+1} using equation (12), where the step size α is chosen by line search.

Stop until the convergence criterion is met. Let t_{max} be the final iteration number.

Output: $\mathbf{T}_{t_{max}}$.

convergence when $p = 1$ and super-linear convergence when $0 < p < 1$.

We remark on the choice of initial value \mathbf{T}_0 when $0 < p < 1$. As discussed previously in Section 2.2, when $0 < p < 1$, the objective function $Q_p(\hat{\mathbf{A}}\mathbf{T}'^{-1})$ is highly nonconvex, and thus, may contain many stationary points. To avoid the algorithm getting stuck at a local optimum, the choice of \mathbf{T}_0 is important. We recommend trying multiple values of p , starting with $p = 1$. For each value of p , we can use the solution from the previous larger value of p as the initial value \mathbf{T}_0 .

4.2 Comparison with Regularised Estimation

To compare the computation of the proposed rotation method and that of regularised estimation, we also describe a proximal gradient algorithm for the L_1 regularised estimator. The proximal algorithm is a state-of-the-art algorithm for solving non-smooth optimisation problems (Parikh & Boyd, 2014). It can be viewed as a generalisation of projected gradient descent. As will be discussed below, each iteration of the algorithm can be computed easily. In principle, the proximal algorithm can also be applied to the L_p regularised estimator, for $0 < p < 1$. However, it is computationally much more costly than the case when $p = 1$, and thus, will not be discussed here.

The L_1 regularised estimator, also referred to as the Lasso estimator, solves the following optimisation problem

$$\min_{\boldsymbol{\theta}} L(\boldsymbol{\Sigma}(\boldsymbol{\theta})) + \gamma \sum_{j=1}^J \sum_{k=1}^K |\lambda_{jk}|.$$

To apply the proximal gradient algorithm, we reparameterise the covariance matrix $\boldsymbol{\Phi}$ by $\mathbf{T}'\mathbf{T}$, and reparameterise the diagonal entries of the diagonal matrix $\boldsymbol{\Omega}$ by $\mathbf{v} = (v_1, \dots, v_J)$, where $v_i = \log(\omega_{ii})$. With slight abuse of notation, we can write the optimisation problem as

$$\min_{\boldsymbol{\Lambda}, \mathbf{T}, \mathbf{v}} L(\boldsymbol{\Sigma}(\boldsymbol{\Lambda}, \mathbf{T}, \mathbf{v})) + \gamma \sum_{j=1}^J \sum_{k=1}^K |\lambda_{jk}|.$$

We define a proximal operator for the loading matrix as

$$\text{Prox}_{\alpha, \gamma}(\tilde{\boldsymbol{\Lambda}}_t) = \arg \min_{\boldsymbol{\Lambda}} \frac{1}{2} \sum_{j=1}^J \sum_{k=1}^K (\lambda_{jk} - \tilde{\lambda}_{jk}^{(t)})^2 + \alpha \gamma \sum_{j=1}^J \sum_{k=1}^K |\lambda_{jk}|, \quad (13)$$

where $\alpha > 0$ will be a step size and $\tilde{\boldsymbol{\Lambda}}_t = (\tilde{\lambda}_{jk}^{(t)})_{J \times K}$ will be the value of $\boldsymbol{\Lambda}$ from the previous step in the proximal gradient algorithm. Note that (13) has a closed-form solution given by soft-thresholding (Parikh

& Boyd, 2014) that can be easily computed. We summarise the proximal gradient algorithm in Algorithm 4 below.

Algorithm 4 Proximal gradient algorithm for L^1 regularised estimation.

Input: The initial values $\mathbf{\Lambda}_0$, \mathbf{T}_0 , and \mathbf{v}_0 .

For iterations $t = 0, 1, 2, \dots$, we iterate between the following two steps:

Step 1: Calculate the gradients of $L(\mathbf{\Sigma}(\mathbf{\Lambda}, \mathbf{T}, \mathbf{v}))$ with respect to $\mathbf{\Lambda}$, \mathbf{T} , and \mathbf{v} , respectively, at $(\mathbf{\Lambda}_t, \mathbf{T}_t, \mathbf{v}_t)$. Denote these gradients by $\nabla L_{t,\mathbf{\Lambda}}$, $\nabla L_{t,\mathbf{T}}$, and $\nabla L_{t,\mathbf{v}}$.

Step 2: Update the parameters by

$$\mathbf{\Lambda}_{t+1} = \text{Prox}_{\alpha,\gamma}(\mathbf{\Lambda}_t - \alpha \nabla L_{t,\mathbf{\Lambda}}),$$

$$\mathbf{T}_{t+1} = \text{Proj}(\mathbf{T}_t - \alpha \nabla L_{t,\mathbf{T}}),$$

and

$$\mathbf{v}_{t+1} = \mathbf{v}_t - \alpha \nabla L_{t,\mathbf{v}}.$$

Recall that the operator $\text{Proj}(\cdot)$ is defined in (11), and α is a step size chosen by line search.

Stop until the convergence criterion is met. Let t_{max} be the final iteration number.

Output: $(\mathbf{\Lambda}_{t_{max}}, \mathbf{T}_{t_{max}}, \mathbf{v}_{t_{max}})$.

Under suitable conditions, this proximal gradient algorithm converges to stationary points of the objective function, and has local linear convergence rate (Karimi et al., 2016). We notice that when $p = 1$, Algorithms 3 and 4 have similar convergence properties. However, their per-iteration computational complexities are different. In particular, Algorithm 4 involve parameters $\mathbf{\Lambda}$ and \mathbf{v} , which substantially increases its computational complexity. In fact, the per-iteration complexity for Algorithm 3 is $O(K^3 + K^2J)$, while that for Algorithm 4 is $O(J^3 + J^2K + K^2J)$. The difference can be substantial, when J is much larger than K .

5 Simulation Study

5.1 Study I

In this study, we evaluate the performance of $L^{0.5}$ and L^1 rotations, and compare them with some traditional rotation methods and L^1 regularised estimation. Several traditional oblique rotation methods are considered, including the oblimin, quartmin, simplimax, geomin and promax methods. These methods have been considered in the simulation studies in Jennrich (2006). They are implemented using the `GPArotation` package (Bernaards & Jennrich, 2005) in R.

Settings. Two simulation settings are considered, one with $J = 15$ manifest variables and $K = 3$ factors, and the other with $J = 30$ and $K = 5$. The first setting has nine manifest variables that each loads on a single factor (three variables for each factor), and six manifest variables that each loads on two factors. The second setting has 15 manifest variables that each loads on a single factor (three variables for each factor), 10 manifest variables that each loads on two factors, and 5 manifest variables that each loads on three factors. The true model parameters are given in the supplementary material. By numerical evaluations, the true

loading matrices satisfies condition C3 for both $L^{0.5}$ and L^1 criteria. Under each setting, three sample sizes are considered, including $N = 400, 800,$ and 1600 . For each setting and each sample size, we run $B = 500$ independent replications.

Evaluation criteria. We evaluate the proposed method from three aspects. First, we compare all estimators in terms of accuracy of point estimation. Second, we compare the proposed method and the L^1 regularised estimator in terms of their model selection accuracy. Finally, we examine the coverage rate of the proposed method for constructing confidence intervals.

When evaluating the performance of different estimators, we take into account the indeterminacy due to column permutations and sign flips. Let $\tilde{\mathbf{\Lambda}}^{(b)}$ be the loading matrix estimate given by a rotation or regularised estimation method in the b th replication. We then find

$$\hat{\mathbf{\Lambda}}^{(b)} = \arg \min_{\mathbf{\Lambda}} \{ \|\mathbf{\Lambda} - \mathbf{\Lambda}^*\|^2 : \mathbf{\Lambda} = \tilde{\mathbf{\Lambda}}^{(b)} \mathbf{D} \tilde{\mathbf{D}}, \mathbf{D} \in \mathcal{D}_1, \tilde{\mathbf{D}} \in \mathcal{D}_2 \},$$

which is the one closest to the true loading matrix $\mathbf{\Lambda}^*$ among all the loading matrices that are equivalent to $\tilde{\mathbf{\Lambda}}^{(b)}$. Our evaluation criteria are constructed based on $\hat{\mathbf{\Lambda}}^{(b)}$:

1. The accuracy of point estimation is estimated by the mean squared error (MSE):

$$\text{MSE} = \frac{\|\hat{\mathbf{\Lambda}}^{(b)} - \mathbf{\Lambda}^*\|_F^2}{JK},$$

where $\hat{\mathbf{\Lambda}}^{(b)}$ is obtained by a certain rotation or regularisation method in the b -th replication.

2. The model selection accuracy is assessed by the area under the curve (AUC) from the corresponding receiver operating characteristic (ROC) curve. For each threshold c , we compute the average true positive rate ($\overline{\text{TPR}}_c$), which is the proportion of successfully identified non-zero elements in the true loading matrix:

$$\overline{\text{TPR}}_c = \frac{1}{B} \sum_{b=1}^B \frac{\sum_{j,k} \mathbb{1}_{\{\hat{\lambda}_{jk}^{(b,c)} \neq 0, \lambda_{jk}^* \neq 0\}}}{\sum_{j,k} \mathbb{1}_{\{\lambda_{jk}^* \neq 0\}}}, \quad (14)$$

where where $\{\hat{\lambda}_{jk}^{(b,c)}\}_{J \times K} = \hat{\mathbf{\Lambda}}^{(b,c)}$ is the estimated loading matrix in the b -th replication from a CFA model based on $\hat{\mathbf{\Gamma}}_c$ using the maximum likelihood estimator. Similarly, we calculate the average true negative rate ($\overline{\text{TNR}}_c$), which is the success rate of identifying zero elements:

$$\overline{\text{TNR}}_c = \frac{1}{B} \sum_{b=1}^B \frac{\sum_{j,k} \mathbb{1}_{\{\hat{\lambda}_{jk}^{(b,c)} = 0, \lambda_{jk}^* = 0\}}}{\sum_{j,k} \mathbb{1}_{\{\lambda_{jk}^* = 0\}}}. \quad (15)$$

The AUC is consequently calculated by plotting $\overline{\text{TPR}}_c$ against $1 - \overline{\text{TNR}}_c$ by varying the threshold c . We also use the overall selection accuracy, i.e., the true selection rate (TR), to evaluate the model selection procedure described in Algorithm 1. The TR is calculated as

$$\text{TR} = \frac{1}{B} \sum_{b=1}^B \frac{\sum_{j,k} \mathbb{1}_{\{\hat{\lambda}_{jk}^{(b,\hat{c})} \neq 0, \lambda_{jk}^* \neq 0\}} + \sum_{j,k} \mathbb{1}_{\{\hat{\lambda}_{jk}^{(b,\hat{c})} = 0, \lambda_{jk}^* = 0\}}}{JK},$$

where \hat{c} is the BIC selected threshold value from Algorithm 1. Correspondingly, we calculate the TPR

and TNR of the selected model as

$$\text{TPR} = \overline{\text{TPR}}_{\hat{c}} \text{ and } \text{TNR} = \overline{\text{TNR}}_{\hat{c}}.$$

3. The entry-wise 95% confidence interval coverage rate (ECIC) is calculated to evaluate the performance of our post-selection confidence interval procedure in Algorithm 2. For each entry of the loading matrix, the empirical probability of the true loading falling within the estimated confidence interval is calculated as

$$\text{ECIC}_{jk} = \frac{\sum_{b=1}^B \mathbb{1}_{\{\lambda_{jk}^{*(N)} \in (l_{jk}^{(N)}, u_{jk}^{(N)})\}}}{B}.$$

Results on point estimation. In Table 1, the MSE of the estimated loading matrix is presented, for both simulation settings and $N \in \{400, 800, 1600\}$. The first five rows show the results based on traditional oblique rotation criteria, followed by the results of the proposed L^p loss function for two choices of p , and finally those of the Lasso estimator for five choices of γ . For both settings and all sample sizes, geomin performed the best among the traditional rotation methods. The geomin results were very similar to those of L^p rotation and the Lasso estimator with sufficiently small tuning parameter γ . For the Lasso estimator, the MSE increased as γ increased. For L^p rotation, only very small differences were observed between $p = 0.5$ and $p = 1$. In addition, their MSEs were close to those of the Lasso estimator with $\gamma = 0.01$ and $\gamma = 0.05$.

Table 1: MSE obtained by using different rotation criteria under various settings, Study I.

	15 × 3			30 × 5		
	N = 400	N = 800	N = 1600	N = 400	N = 800	N = 1600
Oblimin	0.012	0.007	0.004	0.012	0.008	0.006
Quartimin	0.012	0.007	0.004	0.012	0.008	0.006
Simplimax	0.019	0.017	0.019	0.021	0.019	0.017
Geomin	0.010	0.005	0.002	0.010	0.005	0.002
Promax	0.013	0.007	0.005	0.014	0.009	0.007
$L^{0.5}$ rotation	0.011	0.005	0.003	0.010	0.005	0.002
L^1 rotation	0.010	0.005	0.003	0.009	0.004	0.002
Lasso, $\gamma = 0.01$	0.009	0.004	0.002	0.008	0.003	0.002
Lasso, $\gamma = 0.05$	0.009	0.006	0.005	0.007	0.005	0.004
Lasso, $\gamma = 0.1$	0.017	0.015	0.014	0.012	0.011	0.010
Lasso, $\gamma = 0.2$	0.079	0.076	0.074	0.037	0.034	0.032
Lasso, $\gamma = 0.5$	0.244	0.244	0.244	0.146	0.149	0.150

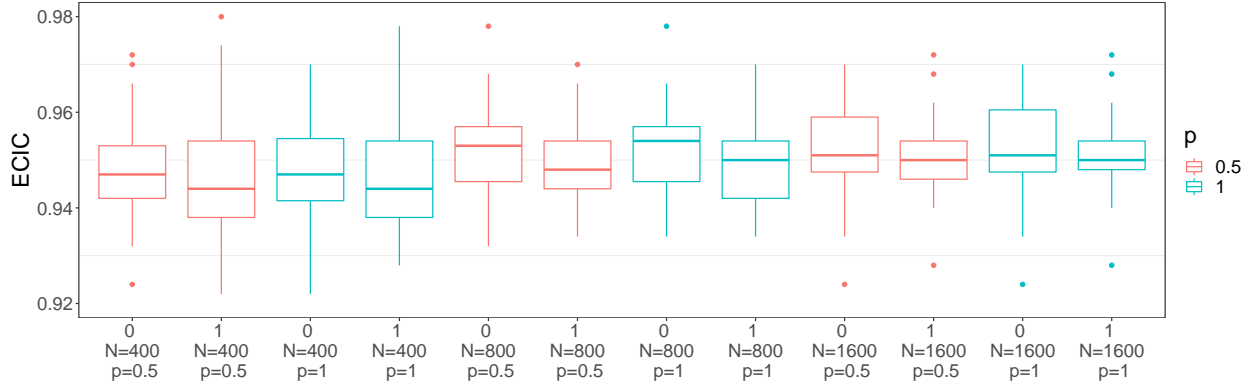
Results on model selection. In Table 2, the AUC, TR, TPR and TNR are presented for the L^p rotations and the Lasso estimator with different tuning parameters. For both scenarios and all sample sizes, the AUC and TR were very similar for the rotation estimator with $p = 0.5$ and $p = 1$. The AUC of the Lasso estimator with a small tuning parameter is similar to that of the L^1 rotation method. We noted that the model selection performance was poor for the Lasso estimator when γ became large. This is due to the presence of many false negative selections (i.e., nonzero loading parameters selected as zeros), as a result of over-regularisation.

Table 2: The AUC, TR, TPR and TNR for the L^p -based rotation estimator and the regularised estimator, Study I.

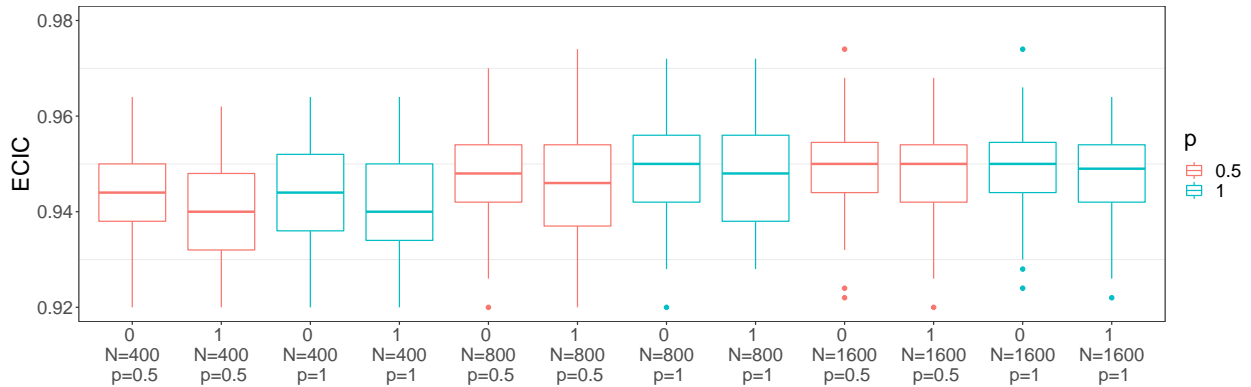
	15×3				30×5			
	AUC	TR	TPR	TNR	AUC	TR	TPR	TNR
$N = 400$								
$L^{0.5}$ rotation	0.996	0.979	0.979	0.979	0.989	0.965	0.93	0.982
L^1 rotation	0.997	0.979	0.979	0.979	0.988	0.964	0.928	0.982
Lasso, $\gamma = 0.01$	0.997	0.981	0.979	0.983	0.989	0.967	0.933	0.984
Lasso, $\gamma = 0.05$	0.997	0.984	0.978	0.989	0.992	0.971	0.937	0.989
Lasso, $\gamma = 0.1$	0.992	0.982	0.973	0.991	0.987	0.969	0.929	0.989
Lasso, $\gamma = 0.2$	0.870	0.848	0.780	0.907	0.904	0.917	0.798	0.977
Lasso, $\gamma = 0.5$	0.500	0.533	0.000	1.000	0.514	0.675	0.053	0.985
$N = 800$								
$L^{0.5}$ rotation	1.000	0.993	0.992	0.993	0.998	0.987	0.978	0.992
L^1 rotation	1.000	0.992	0.993	0.992	0.998	0.987	0.978	0.991
Lasso, $\gamma = 0.01$	1.000	0.992	0.992	0.993	0.998	0.989	0.981	0.993
Lasso, $\gamma = 0.05$	1.000	0.993	0.992	0.993	0.999	0.991	0.982	0.995
Lasso, $\gamma = 0.1$	0.996	0.992	0.988	0.995	0.995	0.989	0.977	0.995
Lasso, $\gamma = 0.2$	0.88	0.861	0.815	0.902	0.919	0.933	0.824	0.987
Lasso, $\gamma = 0.5$	0.500	0.533	0.000	1.000	0.504	0.669	0.019	0.994
$N = 1600$								
$L^{0.5}$ rotation	1.000	0.997	0.999	0.996	1.000	0.997	0.996	0.997
L^1 rotation	1.000	0.997	0.999	0.995	1.000	0.997	0.996	0.997
Lasso, $\gamma = 0.01$	1.000	0.997	1.000	0.995	1.000	0.997	0.997	0.997
Lasso, $\gamma = 0.05$	1.000	0.997	0.999	0.996	1.000	0.997	0.997	0.997
Lasso, $\gamma = 0.1$	0.998	0.997	0.995	0.999	0.998	0.996	0.993	0.998
Lasso, $\gamma = 0.2$	0.886	0.870	0.831	0.904	0.929	0.941	0.838	0.993
Lasso, $\gamma = 0.5$	0.500	0.533	0.000	1.000	0.501	0.667	0.003	0.999

Results on confidence intervals. In Figure 3, boxplots of the ECIC are shown for the L^p rotations, for $p = 0.5$ and $p = 1$ and $N \in \{400, 800, 1600\}$. For both $p = 0.5$ and $p = 1$, the $ECIC_{jks}$ are close to the 95% nominal level, supporting the consistency of the proposed procedure for constructing confidence intervals.

Some remarks. Under the current simulation settings, condition C3 is satisfied by both the $L^{0.5}$ and L^1 criteria, in which cases the two criteria tend to perform similarly. As will be shown in Section 5.2 below, the performance of the two criteria can be substantially different when C3 holds for one criterion but not the other. In addition, we see that the Lasso estimator with a small tuning parameter performed similarly as the L^1 rotation method. This is expected, since the L^1 rotation solution can be viewed as the limiting case of the Lasso estimator when the tuning parameter goes to zero. The Lasso estimator performed poorly for large tuning parameters, due to the bias brought by the regularisation. Finally, it is not clear to us why the geomim rotation performs similarly as the $L^{0.5}$ and L^1 criteria, which is worth future investigation.



(a) Boxplots of $ECIC_{jk}$ for the 15×3 setting



(b) Boxplots of $ECIC_{jk}$ for the 30×5 setting

Figure 3: Boxplots of $ECIC_{jk}$. The label 0 means that $\lambda_{jk}^* = 0$ and the label 1 means that $\lambda_{jk}^* \neq 0$.

5.2 Study II

This study compares the $L^{0.5}$ and L^1 rotations, under a setting where condition C3 holds for the $L^{0.5}$ rotation but not the L^1 rotation. The setting is chosen to somewhat exaggerate the differences, in order to show the consequence of misspecifying p .

Setting and evaluation criteria. The true loading matrix is of dimension $J = 18$ and $K = 3$. Each item is set to load on two factors, so that no item has a perfect simple structure. Given the loading structure, the model is identifiable as a confirmatory factor analysis model. The true model parameters can be found in the supplementary material. By grid search, it is checked that C3 holds for the $L^{0.5}$ criterion but not the L^1 criterion. The sample size is chosen to be $N = 3000$. Similar to Study I, we compare the two rotation criteria using the MSE, AUC, TR, TPR and TNR by running $B = 500$ independent replications.

Results. The results are presented in Table 3. The $L^{0.5}$ criterion performed better in terms of both point estimation and model selection, as its MSE was lower and the AUC, TR, TPR and TNR were higher. In particular, we noted that the $L^{0.5}$ rotation achieved a much higher TNR than the L^1 rotation, meaning that the L^1 rotation tended to make many false positive selections (i.e., zero loading parameters selected as non-zeros), as a consequence of violating condition C3.

Table 3: The MSE, AUC, TR, TPR and TNR for the L^p -based rotation estimator, Study II.

	MSE	AUC	TR	TPR	TNR
$L^{0.5}$ rotation	0.003	0.984	0.951	0.944	0.967
L^1 rotation	0.025	0.954	0.864	0.940	0.712

6 An Application to Big-Five Personality Test

We illustrate the proposed method through an application to the big-five personality test. We consider the Big-Five Factor Markers from the International Personality Item Pool (Goldberg, 1992), which contains 50 items that were designed to measure five personality factors, including Extraversion (E), Emotional Stability (ES), Agreeableness (A), Conscientiousness (C), and Intellect/Imagination (I). Each item is a statement describing a personality pattern like "*I am the life of the party*" and "*I get stressed out easily*", designed to primarily measure one personality factor. The 50 items can be divided into five equal-sized groups, with each group primarily measure one personality factor. Responses to the items are on a five-level Likert scale, which are treated as continuous variables in the current analysis.

Although the big-five personality test was designed to have a perfect simple structure, cross loadings are often found in empirical data (e.g., Gow et al., 2005). To better understand the loading structure of this widely used personality test, we applied the proposed $L^{0.5}$ and L^1 rotations to a dataset² on this test. To avoid possible complexities brought by measurement non-invariance, we selected the subset of male respondents from the United Kingdom, which has a sample size $N = 609$. In the analysis, the number of factors is set to be $K = 5$.

After applying the proposed rotations, we further adjusted the estimates by column permutation and sign flip transformations, so that the resulting factors correspond to the E, ES, A, C, I factors, respectively. Our results are given in Tables 4 through 7. Table 4 shows the estimated covariance matrices from the two rotations. The estimated correlation matrices from the two criteria are similar to each other. In particular, all the signs of the correlations are consistent, except for the correlation between A and I, in which case both correlations are close to zero. In addition, for each pair of factors, the correlations obtained by the two criteria are close. The sign pattern of the correlations between the big-five factors is largely consistent with those found in the literature (e.g., Booth & Hughes, 2014; Gow et al., 2005).

Tables 5 through 7 show the estimated loading parameters and the corresponding 95% confidence intervals obtained from the $L^{0.5}$ rotation. The loadings that are significantly different from zero according to the 95% confidence intervals are indicated by asterisks. The results of the L^1 rotation are similar, and thus, are given in the supplementary material. In Tables 5-7, the items are labelled based on the personality factor that they are designed to measure, and their scoring keys³. The estimated loading matrix is largely consistent with the true loading structure, where all the items have relatively strong loadings on the factors that they are designed to measure, and the signs of the loadings are consistent with the scoring keys. The confidence intervals shed additional light on the uncertainty of each loading. Specifically, we notice that many loadings are statistically insignificantly different from zero, suggesting that the true loading structure is sparse. There are also items with fairly strong cross loadings. For example, item C4 "I make a mess of things" loads strongly on not only factor C, but also factor ES. In fact, its estimated loading on ES is -0.607, with a confidence interval (-0.677, -0.504). This seems to sensible, as item C4 may remind people about stressful situations

²The dataset is downloaded from: http://personality-testing.info/_rawdata/.

³Positively scored items are indicated by "(+)" and negatively scored items are indicated by "(-)".

that are covered by the ES factor. For another example, item ES4 "I seldom feel blue" also loads positively on factor E, with an estimated loading 0.237 and a confidence interval (0.115, 0.310). It also makes sense, as this item seems to be closely related to how energetic a person is.

Table 4: Estimated correlation matrices based on $L^{0.5}$ and L^1 rotations, big-five personality test

	$p = 0.5$					$p = 1$				
	E	ES	A	C	I	E	ES	A	C	I
E	1					1				
ES	0.117	1				0.186	1			
A	0.194	-0.015	1			0.194	-0.002	1		
C	0.005	0.106	0.035	1		0.019	0.144	0.038	1	
I	0.035	0.020	-0.005	-0.028	1	0.161	0.043	0.020	-0.017	1

7 Concluding Remarks

This paper proposes a new family of oblique rotations based on component-wise L^p loss functions ($0 < p \leq 1$) and establishes the relationship between the proposed rotation estimator and the L^p regularised estimator for EFA. Point estimation, model selection, and post-selection inference procedures are developed, and their asymptotic theories are established. An iteratively reweighted gradient projection algorithm is developed for the computation, for which an R package has been developed and will be published on Github upon the acceptance of this paper. The package is also available to reviewers upon request. The power of the proposed method is demonstrated via simulation studies and an application to big-five personality assessment.

We note that the proposed procedures do not rely on the normality assumption of the EFA model, though such an assumption is made in the problem setup for the ease of exposition. Specifically, in the rotation, one only needs to obtain a consistent initial estimator for EFA in the sense of condition C1, which can be obtained with any reasonable loss function for factor analysis. In the model selection, only the BIC uses the likelihood function based on the normal model. Note that the likelihood function is a valid loss function under the linear factor model, even if the normality assumption does not hold (Chapter 7, Bollen, 1989). Therefore, the BIC still yields consistent model selection under the misspecification of the normality assumption (Machado, 1993). Finally, the confidence intervals are based on the asymptotic distributions of CFA models. If we use a robust method (i.e., a sandwich estimator) for computing the asymptotic variance, then the resulting confidence intervals are valid when the normality assumption does not hold.

From the previous discussion, we see that there is a statistical and computational trade-off underlying the choice of p . Theoretically, a smaller value of p is more likely to recover a sparse loading matrix, but the associated optimisation problem is computationally more challenging. Our recommendation is to try multiple values of p , starting from $p = 1$ and gradually decreasing the value of p . Computationally, when solving the optimisation with a smaller value of p , we recommend using the solution from the previous larger value of p as the starting point, so that the algorithm is less likely to get stuck at a local optimum. Then, one may compare these solutions based on their model selection results using the BIC or other criteria for model comparison.

Our complexity analysis and simulation results suggest that obtaining a solution path for L^1 regularised estimator has little added value over the L^1 rotation, at least when the sample size is reasonably large.

Table 5: Part I: Point estimates and confidence intervals constructed by $L^{0.5}$, big-five personality test. The loadings that are significantly different from zero according to the 95% confidence intervals are indicated by asterisks.

	E	ES	A	C	I
E1(+)	0.882* (0.793, 0.980)	-0.055 (-0.161, 0.003)	-0.068* (-0.183,-0.017)	0.015 (-0.078, 0.100)	0.087* (0.005, 0.170)
E2(-)	-0.845* (-0.962,-0.760)	0.117* (0.048, 0.228)	0.002 (-0.057, 0.126)	0.031 (-0.061, 0.132)	-0.020 (-0.104, 0.079)
E3(+)	0.786* (0.702, 0.876)	0.286* (0.192, 0.347)	0.203* (0.120, 0.275)	0.123* (0.050, 0.213)	-0.088* (-0.175,-0.020)
E4(-)	-0.913* (-1.019,-0.842)	-0.072 (-0.140, 0.011)	-0.022 (-0.075, 0.077)	0.000 (-0.099, 0.068)	0.084* (0.033, 0.184)
E5(+)	0.895* (0.812, 0.987)	-0.012 (-0.118, 0.032)	0.155* (0.059, 0.209)	0.104* (0.023, 0.183)	0.085* (0.021, 0.172)
E6(-)	-0.751* (-0.849,-0.660)	-0.011 (-0.069, 0.103)	-0.088 (-0.163, 0.010)	-0.062 (-0.161, 0.022)	-0.141* (-0.226,-0.052)
E7(+)	1.114* (1.020, 1.221)	-0.062* (-0.189,-0.018)	0.083* (0.001, 0.172)	0.105* (0.020, 0.199)	-0.015 (-0.117, 0.052)
E8(-)	-0.722* (-0.823,-0.630)	-0.099* (-0.176, 0.000)	0.028 (-0.038, 0.140)	0.118* (0.024, 0.210)	-0.069 (-0.157, 0.022)
E9(+)	0.858* (0.748, 0.953)	0.064 (-0.054, 0.131)	0.000 (-0.111, 0.075)	-0.013 (-0.110, 0.086)	0.246* (0.145, 0.332)
E10(-)	-0.829* (-0.930,-0.741)	-0.128* (-0.193,-0.025)	-0.048 (-0.123, 0.047)	-0.121* (-0.215,-0.036)	0.000 (-0.078, 0.092)
ES1(-)	-0.152* (-0.210,-0.028)	-0.975* (-1.073,-0.875)	0.008 (-0.121, 0.078)	0.081* (0.016, 0.200)	-0.104* (-0.193,-0.017)
ES2(+)	0.161* (0.039, 0.215)	0.675* (0.589, 0.771)	0.000 (-0.064, 0.115)	-0.084* (-0.197,-0.020)	0.085* (0.012, 0.185)
ES3(-)	-0.203* (-0.271,-0.093)	-0.786* (-0.881,-0.696)	0.232* (0.124, 0.304)	0.122* (0.031, 0.208)	0.042 (-0.033, 0.139)
ES4(+)	0.237* (0.115, 0.310)	0.568* (0.474, 0.670)	0.001 (-0.069, 0.125)	0.066 (-0.049, 0.148)	0.011 (-0.079, 0.113)
ES5(-)	0.004 (-0.073, 0.138)	-0.471* (-0.567,-0.357)	-0.041 (-0.163, 0.046)	-0.110 (-0.208, 0.006)	-0.225* (-0.345,-0.135)
ES6(-)	-0.147* (-0.202,-0.022)	-0.808* (-0.905,-0.717)	0.259* (0.145, 0.327)	-0.025 (-0.106, 0.074)	-0.132* (-0.227,-0.053)
ES7(-)	0.000 (-0.048, 0.123)	-0.962* (-1.064,-0.883)	-0.111* (-0.226,-0.055)	-0.044 (-0.102, 0.064)	0.004 (-0.089, 0.071)
ES8(-)	-0.026 (-0.080, 0.106)	-1.130* (-1.240,-1.046)	-0.133* (-0.261,-0.080)	-0.076 (-0.140, 0.036)	0.000 (-0.103, 0.065)
ES9(-)	-0.051 (-0.131, 0.048)	-0.866* (-0.956,-0.768)	-0.292* (-0.399,-0.214)	0.171* (0.092, 0.267)	-0.018 (-0.104, 0.068)
ES10(-)	-0.364* (-0.435,-0.256)	-0.842* (-0.940,-0.752)	0.070 (-0.029, 0.155)	-0.109* (-0.181,-0.004)	0.096* (0.016, 0.187)

Table 6: Part II: Point estimates and confidence intervals constructed by $L^{0.5}$, big-five personality test.

	E	ES	A	C	I
A1(-)	0.000 (-0.112, 0.088)	-0.127* (-0.205,-0.013)	-0.779* (-0.876,-0.670)	0.030 (-0.071, 0.127)	0.044 (-0.060, 0.134)
A2(+)	0.437* (0.359, 0.523)	0.000 (-0.099, 0.053)	0.557* (0.464, 0.626)	-0.043 (-0.124, 0.034)	0.046 (-0.026, 0.128)
A3(-)	0.178* (0.080, 0.286)	-0.571* (-0.674,-0.467)	-0.565* (-0.692,-0.480)	-0.077 (-0.177, 0.030)	0.138* (0.029, 0.231)
A4(+)	0.013 (-0.034, 0.142)	0.000 (-0.100, 0.039)	0.980* (0.895, 1.050)	-0.015 (-0.098, 0.032)	0.000 (-0.060, 0.071)
A5(-)	-0.156* (-0.248,-0.088)	-0.041 (-0.105, 0.047)	-0.815* (-0.894,-0.725)	0.000 (-0.078, 0.077)	0.086* (0.011, 0.163)
A6(+)	-0.063 (-0.157, 0.020)	-0.184* (-0.270,-0.102)	0.717* (0.630, 0.812)	0.007 (-0.100, 0.073)	0.014 (-0.073, 0.096)
A7(-)	-0.367* (-0.452,-0.297)	-0.095* (-0.161,-0.015)	-0.733* (-0.800,-0.640)	0.057 (-0.016, 0.133)	0.026 (-0.047, 0.098)
A8(+)	0.110* (0.039, 0.185)	-0.038 (-0.128, 0.011)	0.692* (0.616, 0.770)	0.079* (0.007, 0.149)	0.028 (-0.034, 0.106)
A9(+)	0.119* (0.040, 0.199)	-0.111* (-0.206,-0.055)	0.752* (0.667, 0.835)	0.064 (-0.015, 0.140)	0.114* (0.042, 0.194)
A10(+)	0.440* (0.352, 0.515)	0.075 (-0.008, 0.145)	0.321* (0.244, 0.401)	0.125* (0.033, 0.193)	0.056 (-0.019, 0.136)
C1(+)	0.111* (0.002, 0.180)	0.101 (-0.003, 0.179)	-0.037 (-0.108, 0.079)	0.686* (0.583, 0.771)	0.131* (0.064, 0.244)
C2(-)	0.070 (-0.015, 0.191)	-0.190* (-0.285,-0.078)	0.108 (-0.020, 0.185)	-0.658* (-0.793,-0.581)	0.145* (0.012, 0.215)
C3(+)	0.024 (-0.078, 0.083)	0.000 (-0.094, 0.066)	0.114* (0.046, 0.206)	0.401* (0.300, 0.465)	0.280* (0.217, 0.379)
C4(-)	-0.140* (-0.201,-0.036)	-0.607* (-0.677,-0.504)	0.049 (-0.052, 0.116)	-0.496* (-0.576,-0.407)	-0.041* (-0.170,-0.006)
C5(+)	0.081* (0.001, 0.192)	0.046 (-0.047, 0.161)	0.000 (-0.053, 0.151)	0.779* (0.691, 0.887)	-0.051 (-0.126, 0.066)
C6(-)	0.011 (-0.088, 0.124)	-0.184* (-0.277,-0.062)	0.046 (-0.078, 0.139)	-0.705* (-0.841,-0.621)	0.089 (-0.024, 0.188)
C7(+)	-0.129* (-0.221,-0.044)	-0.139* (-0.235,-0.057)	0.110* (0.035, 0.214)	0.528* (0.434, 0.618)	0.038 (-0.021, 0.157)
C8(-)	-0.010 (-0.087, 0.094)	-0.275* (-0.355,-0.173)	-0.241* (-0.356,-0.174)	-0.524* (-0.608,-0.421)	0.000 (-0.122, 0.059)
C9(+)	0.036 (-0.058, 0.130)	-0.014 (-0.134, 0.067)	0.123* (0.052, 0.241)	0.723* (0.626, 0.821)	-0.076 (-0.149, 0.040)
C10(+)	0.000 (-0.107, 0.059)	-0.016 (-0.117, 0.051)	0.128* (0.065, 0.231)	0.524* (0.416, 0.587)	0.234* (0.172, 0.337)

Table 7: Part III: Point estimates and confidence intervals constructed by $L^{0.5}$, big-five personality test.

	E	ES	A	C	I
I1(+)	0.079 (-0.021, 0.145)	0.000 (-0.109, 0.057)	-0.045 (-0.146, 0.014)	0.000 (-0.108, 0.056)	0.623* (0.544, 0.711)
I2(-)	0.000 (-0.051, 0.121)	-0.220* (-0.283,-0.114)	-0.087* (-0.183,-0.015)	0.009 (-0.055, 0.117)	-0.581* (-0.675,-0.502)
I3(+)	0.067 (-0.026, 0.135)	-0.153* (-0.251,-0.092)	0.025 (-0.061, 0.096)	0.002 (-0.098, 0.063)	0.589* (0.502, 0.665)
I4(-)	0.024 (-0.027, 0.144)	-0.202* (-0.267,-0.098)	-0.154* (-0.230,-0.064)	0.036 (-0.022, 0.148)	-0.571* (-0.660,-0.487)
I5(+)	0.237* (0.133, 0.271)	0.067 (-0.002, 0.137)	-0.058 (-0.132, 0.002)	0.176* (0.069, 0.205)	0.581* (0.509, 0.651)
I6(-)	-0.211* (-0.272,-0.102)	-0.003 (-0.060, 0.108)	-0.047 (-0.121, 0.044)	0.028 (-0.038, 0.133)	-0.510* (-0.605,-0.434)
I7(+)	0.076 (-0.017, 0.123)	0.166* (0.084, 0.221)	-0.035 (-0.100, 0.036)	0.097* (0.012, 0.153)	0.450* (0.382, 0.524)
I8(+)	-0.024 (-0.163, 0.021)	-0.165* (-0.270,-0.090)	-0.107* (-0.197,-0.020)	0.000 (-0.123, 0.060)	0.656* (0.577, 0.764)
I9(+)	-0.063 (-0.153, 0.008)	-0.217* (-0.309,-0.151)	0.240* (0.156, 0.315)	0.107* (0.017, 0.179)	0.258* (0.183, 0.343)
I10(+)	0.240* (0.132, 0.275)	-0.004 (-0.113, 0.036)	0.000 (-0.072, 0.068)	0.097* (0.012, 0.155)	0.685* (0.613, 0.762)

That is, obtaining the solution path of the regularised estimator is computationally more intensive, while the best tuning parameter is often very close to zero and thus the corresponding solution is very similar to the rotation solution. Therefore, when the sample size is reasonably large, we do not recommend running a solution path for the L^1 regularised estimator to learn the loading structure in EFA. Instead, one can obtain a point estimate by either applying the L^1 rotation or running the L^1 regularised estimator with a single small tuning parameter. Model selection can be done by applying hard-thresholding to this point estimate. Furthermore, although an L^p regularised estimator is mathematically well-defined with $p < 1$, algorithms remain to be developed for its computation. On the other hand, L^p rotation can be computed by the proposed IRGP algorithm, for all $p \in (0, 1]$.

The current work has several limitations that require future investigations. First, the way the confidence intervals are constructed may be improved. That is, accurate model selection (condition C5) and identifiability conditions on the true model (condition C6) are required for the confidence intervals to have good coverage rate, while the uncertainty in the model selection step is not taken into account in the proposed procedure. Consequently, although the proposed confidence intervals are shown to be asymptotically valid, they may not perform well when the sample size is small. This issue may be addressed by developing bootstrap procedures for constructing confidence intervals, as bootstrap procedures may still be valid even when the objective function is non-smooth (Sen et al., 2010).

The current theoretical results only consider a low-dimensional setting where the numbers of manifest variables and factors are fixed and the sample size goes to infinity. As factor analysis is commonly used to analyse high-dimensional multivariate data, it is of interest to generalise the current results to a high-dimensional regime where the numbers of manifest variables, factors, and observations all grow to infinity (Chen & Li, 2022; Chen et al., 2019, 2020; Zhang et al., 2020). In particular, it will be of interest to see how the rotation methods work with the joint maximum likelihood estimator for high-dimensional factor models (Chen et al., 2019, 2020).

Finally, as an issue with any simulation study, we can only examine a small number of simulation settings, and thus, may not be able to provide a complete picture about the proposed methods. More simulation settings need to be investigated, by varying the numbers of manifest variables, factors, and observations, the sign pattern of the true loading matrix, and the generation mechanism of the true model parameters. This is left for future investigation.

References

- Ba, D., Babadi, B., Purdon, P. L., & Brown, E. N. (2013). Convergence and stability of iteratively re-weighted least squares algorithms. *IEEE Transactions on Signal Processing*, *62*(1), 183–195.
- Bartholomew, D. J., Knott, M., & Moustaki, I. (2011). *Latent variable models and factor analysis: A unified approach*. John Wiley & Sons.
- Bernaards, C. A., & Jennrich, R. I. (2005). Gradient projection algorithms and software for arbitrary rotation criteria in factor analysis. *Educational and Psychological Measurement*, *65*(5), 676–696.
- Bollen, K. A. (1989). *Structural equations with latent variables*. John Wiley & Sons.
- Booth, T., & Hughes, D. J. (2014). Exploratory structural equation modeling of personality data. *Assessment*, *21*(3), 260–271.

- Browne, M. W. (1984). Asymptotically distribution-free methods for the analysis of covariance structures. *British Journal of Mathematical and Statistical Psychology*, *37*(1), 62–83.
- Chen, Y., & Li, X. (2022). Determining the number of factors in high-dimensional generalized latent factor models. *Biometrika*, to appear.
- Chen, Y., Li, X., Liu, J., & Ying, Z. (2021). Item response theory—a statistical framework for educational and psychological measurement. *arXiv preprint arXiv:2108.08604*.
- Chen, Y., Li, X., & Zhang, S. (2019). Joint maximum likelihood estimation for high-dimensional exploratory item factor analysis. *Psychometrika*, *84*(1), 124–146.
- Chen, Y., Li, X., & Zhang, S. (2020). Structured latent factor analysis for large-scale data: Identifiability, estimability, and their implications. *Journal of the American Statistical Association*, *115*(532), 1756–1770.
- Choi, J., Oehlert, G., & Zou, H. (2010). A penalized maximum likelihood approach to sparse factor analysis. *Statistics and its Interface*, *3*(4), 429–436.
- Daubechies, I., DeVore, R., Fornasier, M., & Güntürk, C. S. (2010). Iteratively reweighted least squares minimization for sparse recovery. *Communications on Pure and Applied Mathematics: A Journal Issued by the Courant Institute of Mathematical Sciences*, *63*(1), 1–38.
- Dempster, A. P., Laird, N. M., & Rubin, D. B. (1977). Maximum likelihood from incomplete data via the em algorithm. *Journal of the Royal Statistical Society: Series B (Methodological)*, *39*(1), 1–22.
- Geminiani, E., Marra, G., & Moustaki, I. (2021). Single-and multiple-group penalized factor analysis: A trust-region algorithm approach with integrated automatic multiple tuning parameter selection. *Psychometrika*, *86*(1), 65–95.
- Goldberg, L. R. (1992). The development of markers for the big-five factor structure. *Psychological Assessment*, *4*(1), 26.
- Gow, A. J., Whiteman, M. C., Pattie, A., & Deary, I. J. (2005). Goldberg’s ‘ipip’big-five factor markers: Internal consistency and concurrent validation in scotland. *Personality and Individual Differences*, *39*(2), 317–329.
- Hirose, K., & Yamamoto, M. (2014). Estimation of an oblique structure via penalized likelihood factor analysis. *Computational Statistics & Data Analysis*, *79*, 120–132.
- Hirose, K., & Yamamoto, M. (2015). Sparse estimation via nonconcave penalized likelihood in factor analysis model. *Statistics and Computing*, *25*(5), 863–875.
- Jennrich, R. I. (1973). Standard errors for obliquely rotated factor loadings. *Psychometrika*, *38*(4), 593–604.
- Jennrich, R. I. (2002). A simple general method for oblique rotation. *Psychometrika*, *67*(1), 7–19.
- Jennrich, R. I. (2004). Rotation to simple loadings using component loss functions: The orthogonal case. *Psychometrika*, *69*(2), 257–273.
- Jennrich, R. I. (2006). Rotation to simple loadings using component loss functions: The oblique case. *Psychometrika*, *71*(1), 173–191.
- Jennrich, R. I., & Sampson, P. (1966). Rotation for simple loadings. *Psychometrika*, *31*(3), 313–323.
- Jin, S., Moustaki, I., & Yang-Wallentin, F. (2018). Approximated penalized maximum likelihood for exploratory factor analysis: An orthogonal case. *Psychometrika*, *83*(3), 628–649.
- Jöreskog, K. G. (1967). Some contributions to maximum likelihood factor analysis. *Psychometrika*, *32*(4), 443–482.
- Jöreskog, K. G., & Goldberger, A. S. (1972). Factor analysis by generalized least squares. *Psychometrika*, *37*(3), 243–260.

- Kaiser, H. F. (1958). The varimax criterion for analytic rotation in factor analysis. *Psychometrika*, 23(3), 187–200.
- Karimi, H., Nutini, J., & Schmidt, M. (2016). Linear convergence of gradient and proximal-gradient methods under the polyak-łojasiewicz condition. *Joint European Conference on Machine Learning and Knowledge Discovery in Databases*, 795–811.
- Kiers, H. A. (1994). Simplicimax: Oblique rotation to an optimal target with simple structure. *Psychometrika*, 59(4), 567–579.
- Lai, M.-J., & Wang, J. (2011). An unconstrained ℓ_q minimization with $0 < q \leq 1$ for sparse solution of underdetermined linear systems. *SIAM Journal on Optimization*, 21(1), 82–101.
- Machado, J. A. (1993). Robust model selection and m-estimation. *Econometric Theory*, 9(3), 478–493.
- Mazumder, R., Friedman, J. H., & Hastie, T. (2011). Sparsenet: Coordinate descent with nonconvex penalties. *Journal of the American Statistical Association*, 106(495), 1125–1138.
- Meinshausen, N., & Yu, B. (2009). Lasso-type recovery of sparse representations for high-dimensional data. *The Annals of Statistics*, 37(1), 246–270.
- Mulaik, S. A. (2009). *Foundations of factor analysis*. CRC press.
- Parikh, N., & Boyd, S. (2014). Proximal algorithms. *Foundations and Trends in Optimization*, 1(3), 127–239.
- Reckase, M. D. (2009). Multidimensional item response theory models. *Multidimensional item response theory* (pp. 79–112). Springer.
- Rohe, K., & Zeng, M. (2022). Vintage factor analysis with varimax performs statistical inference. *Journal of the Royal Statistical Society - Series B*, to appear.
- Schwarz, G. (1978). Estimating the dimension of a model. *The Annals of Statistics*, 461–464.
- Sen, B., Banerjee, M., & Woodroffe, M. (2010). Inconsistency of bootstrap: The grenander estimator. *The Annals of Statistics*, 38(4), 1953–1977.
- Shao, J. (1997). An asymptotic theory for linear model selection. *Statistica Sinica*, 221–242.
- Thurstone, L. L. (1947). *Multiple-factor analysis; a development and expansion of the vectors of mind*. University of Chicago Press.
- Trendafilov, N. T. (2014). From simple structure to sparse components: A review. *Computational Statistics*, 29(3), 431–454.
- Vrieze, S. I. (2012). Model selection and psychological theory: A discussion of the differences between the akaike information criterion (aic) and the bayesian information criterion (bic). *Psychological Methods*, 17(2), 228.
- Yamamoto, M., Hirose, K., & Nagata, H. (2017). Graphical tool of sparse factor analysis. *Behaviormetrika*, 44(1), 229–250.
- Yates, A. (1987). *Multivariate exploratory data analysis: A perspective on exploratory factor analysis*. Suny Press.
- Zhang, H., Chen, Y., & Li, X. (2020). A note on exploratory item factor analysis by singular value decomposition. *Psychometrika*, 85(2), 358–372.
- Zhao, S., Witten, D., & Shojaie, A. (2021). In defense of the indefensible: A very naive approach to high-dimensional inference. *Statistical Science*, 36(4), 562–577.
- Zheng, L., Maleki, A., Weng, H., Wang, X., & Long, T. (2017). Does l_p -minimization outperform l_1 -minimization? *IEEE Transactions on Information Theory*, 63(11), 6896–6935.